Electrochemical Membrane Process for Flue Gas Desulfurization

Dennis J. McHenry and Jack Winnick
School of Chemical Engineering, Georgia Institute of Technology, Atlanta, GA 30332

A flue gas desulfurization process being developed for coal-fired power plants removes and concentrates sulfur oxides (SO_x). The key element is an electrochemical cell using a sulfur oxide selective membrane. It achieves 90% sulfur oxide removal with near 100% electric current efficiency.

Recent research has focused on improving the structure of the electrochemical membrane and its interface with the electrodes. The capillary forces of the membrane and porous electrodes establish an equilibrium. To maintain electrode surface area enhancement, it is necessary to retain the electrolyte in the membrane and allow only wetting of the electrode pores. Chemically-stable matrix materials for the membrane have been identified; several fabrication techniques were used to prepare the actual membrane structure. A new electrode material, $(LiO)_xNiO$, possesses the proper chemical stability and electrical properties in the corrosive environment. These modifications have led to an order of magnitude increase in flux and operating lifetime.

Introduction

A large number of flue gas desulfurization processes are presently under development throughout the world to combat the acid rain problem with most using wet or dry sorption to preferentially remove SO_2 from the flue gas. Most of these processes need expensive reagents, a flue gas reheating step and a landfill for disposal of the captured sulfur. This leads to high operating and capital costs. With the recent 1991 Clean Air Act, these processes will see continued interest as utilities attempt to reduce SO_2 emissions by 10 million tons from 1980 levels.

Here we present the development of an electrochemical membrane flue gas desulfurization process, which overcomes the problems of most other flue gas desulfurization processes. As a membrane separation process, it has similarities to other membrane processes, with one major difference: the driving force for the separation is an applied electric field instead of a conventional pressure or concentration gradient. This technique has been applied to other separation schemes, such as the production of oxygen from air (Langer and Haldeman, 1964), the removal of carbon dioxide from dilute streams (Kang and Winnick, 1985; Walke et al., 1988) and hydrogen sulfide from coal gas (Weaver and Winnick, 1991) or natural gas (Alexander and Winnick, 1990). The key is that the components to be removed must be the strongest electron acceptors (Lewis acids) in the gas mixture. Sulfur oxides are the most acidic of all species present in flue gas and are therefore theoretically separable by this technique.

When development is complete, this technique offers several advantages over standard limestone scrubbing. The operation is continuous and totally *in situ*; no liquid is pumped and no regeneration is required. No reagents are necessary, other than about 1-2% of the plant electric power production. Furthermore, a salable byproduct, oleum, (anhydrous sulfuric acid) is produced; no waste is emitted. Finally, operation at flue-gas temperature eliminates the need for stack-gas-reheat.

While the goal of process development is to produce a process for the removal of SO_x and NO_x, the focus of this article is on the SO_x removal capabilities.

Background

The heart of the process is the electrolyte-filled membrane sandwiched between the two porous, gas-diffusion electrodes,

Correspondence concerning this article should be addressed to J. Winnick.
Current address of D. J. McHenry, Westvaco Corporation, Charleston Research Center, P.O. Box 2941105, N. Charleston, SC 29411.

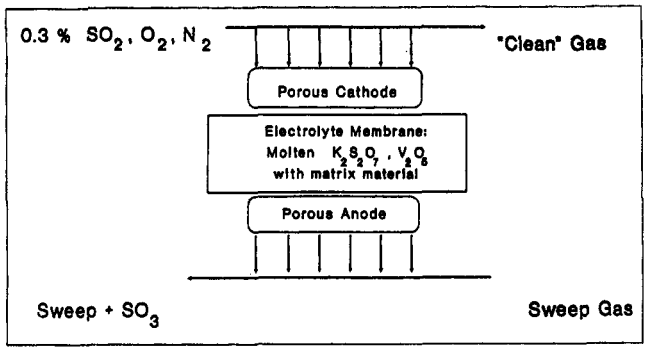

Figure 1. Electrochemical SO_x removal process.

which impose the required voltage gradient across the cell and initiate the required electrochemistry. Preoxidized flue gas enters the cathode side and diffuses into the pores of the electrode, where a series of reactions selectively remove SO_3 at the cathode/membrane interface and generate SO_3 at the anode/membrane interface. The SO_3 diffuses out of the anode and is carried away as a concentrated byproduct stream, to undergo further processing to sulfuric acid (H_2SO_4) or oleum ($H_2S_2O_7$). Figure 1 shows the removal process.

Process chemistry

The initial development work (Townley and Winnick, 1981, 1983) utilized the ternary lithium-sodium-potassium sulfate eutectic as the electrolyte ($T_{mp}=512°C$) and confirmed the feasibility of the scheme. This cell showed removals in excess of 95% of the inlet SO_x from simulated flue gas. Unfortunately, the high melting temperature of this electrolyte made retrofit to existing coal-fired utilities difficult. Ideally, flue gas processes should operate at less than 400°C, the temperature of flue gas exiting the power plant economizer.

Scott (1985) identified an alternate low-melting electrolyte as potassium pyrosulfate ($K_2S_2O_7$) with small additions of K_2SO_4 and V_2O_5. This electrolyte melts near 285°C, depending on the level of V_2O_5 present, and is stable to temperatures in excess of 400°C. Free-electrolyte studies (Scott et al., 1988) and (Franke and Winnick, 1989a) showed the cathodic reaction to be the direct reduction of pyrosulfate and the stepwise SO_x removal to be:

$$2S_2O_7^{2-} + 2e^- \rightarrow 3SO_4^{2-} + SO_2 \tag{1}$$

$$SO_2 + \frac{1}{2}O_2 \xrightarrow{V_2O_5} SO_3 \tag{2}$$

$$2SO_3 + 2SO_4^{2-} \rightarrow 2S_2O_7^{2-} \tag{3}$$

Complete details and half-wave potentials can be found in the references. One of the two sulfur trioxides comes from the gas phase, to effect the actual removal. Note that the actual SO_x removal reaction (reaction 3) is a gas/liquid two-phase reaction; hence, its rate is strongly determined by the available interfacial area. The overall cathodic reaction is determined by summing these equations to yield:

$$SO_3 + \frac{1}{2}O_2 + 2e^- \rightarrow SO_4^{2-} \tag{4}$$

The resulting sulfate ion is transported to the anode by the imposed electrical field, where it is oxidized to the thermodynamically-favored species:

$$SO_4^{2-} \rightarrow SO_3 + \frac{1}{2}O_2 + 2e^- \tag{5}$$

The two half-cell reactions, when summed, show there is no net electrolyte reaction, but rather a transport of SO_x (and some oxygen) from the cathode to the anode:

$$\left(SO_3 + \frac{1}{2}O_2\right)_{\text{cathode}} \rightarrow \left(SO_3 + \frac{1}{2}O_2\right)_{\text{anode}} \tag{6}$$

The transport of oxygen and its presence in the anode gas stream is of minor consequence in a fully oxidized gas stream.

Early removal studies showed the gas-phase oxidation of SO_2 (reaction 2) to be the rate determining step. To remove this limitation, two catalysts have been identified. In laboratory studies, a 2% platinum-on-silica-gel catalyst is used to chemically preoxidize the SO_2 before it enters the removal cell. At 400°C, this catalyst converts 99% of the SO_2. For larger applications, a commercial sulfuric acid catalyst, for example, Haldor-Topsøe VK38, would be used upstream of the removal stacks. Additionally, for laboratory studies below 400°C, the oxidation kinetics over platinum decrease, and to ensure complete conversion of SO_2 to SO_3, an external SO_2 preoxidation reactor filled with Haldor-Topsøe VK38 is operated at 400°C upstream of the removal cell.

For complete removal of SO_2, the electrochemically generated SO_2 (see reaction 1) must be oxidized in the electrolyte by V_2O_5. Inclusion of 1 wt. % of V_2O_5 allowed Franke and Winnick (1989b) to reach greater than 95% removal of SO_3 for a flow rate of 100 mL/min (0.3% SO_2, 3.0% O_2, balance N_2) at 100% current efficiency. As currents increase, the rate of electrochemical generation of SO_2 (reaction 1) may exceed the rate of SO_2 oxidation by V_2O_5 in the electrolyte. This situation reduces the amount of SO_3 available to neutralize excess sulfate and causes increased polarization at the anode due to the high level of sulfate in the electrolyte. After sufficient time, the sulfate content exceeds its solubility limit (~6%), and the anolyte film freezes, reducing ionic conductivity.

Electrolyte membrane

In the electrolyte membrane, a matrix of particles is used to immobilize the molten electrolyte with matrix interstitial spaces retaining the electrolyte through capillarity. Since a porous electrode is on each side of the membrane and exerts its own capillarity, membrane capillarity must exceed that of the electrode pores in order to prevent the electrolyte from leaking out of the membrane and filling the electrodes. However, there should be a thin film of electrolyte on the electrode pore walls to maximize the gas/electrolyte interfacial area. When this condition is not met, polarization performance suffers; more driving force is required to achieve the same separation.

Arendt and Curran (1980) found that poor polarization per-

formance in the molten carbonate fuel cell (MCFC) was due in large measure to flooding of the electrodes with molten electrolyte resulting from excessive overlap of the matrix and electrode pore distributions. To prevent this, the matrix interstice size distribution should be one order of magnitude smaller than the electrode pores. Arendt (1982) later states that the matrix material and resulting membrane must:

(i) Be chemically and physically stable for extended periods
(ii) Provide an appropriate interstice size distribution, stable in time, to complement the electrode structures, thereby providing optimum electrochemical performance
(iii) Be of minimum crystallite size, consistent with the stability and interstice distribution criteria to maximize the liquid electrolyte volume fraction and ionic conductivity of the membrane.

These criteria are required in the SO_x electrochemical removal system, as well for optimum performance.

In the initial configuration of the SO_x removal process, Franke and Winnick (1989a) used MgO as the matrix material of choice. The resulting membranes showed excellent SO_x removal, but polarization was higher than expected, relative to MCFC results. This deficiency is due to leakage of electrolyte from the membrane into the electrode pores. Franke found the MgO to react with the electrolyte during processing to form a stable matrix, $K_2Mg_2(SO_4)_3$. The reaction products were fabricated into a membrane by first drying the powder, pressing under 137 bar (2,000 psi) in a hydraulic ram, heating to 270°C for 3 h and repressing at 137 bar. This hot pressing technique produced 1–1.5-mm-thick membranes with greater than 95% of theoretical density.

Because the actual SO_3 removal reaction (reaction 3) is due to a gas-liquid reaction, it is heavily dependent on exposed liquid surface area. Observations of MgO-based membranes showed a two-order-of-magnitude loss in interfacial area, which related closely to the drop in mass flux. Part of this work has focused on reducing the size of the matrix interstices, thereby decreasing the level of electrode-pore flooding.

Electrodes

Several electrode materials have been used during the development of this process. In the ternary sulfate electrolyte, at 600°C, Townley found NiO electrodes to react to the nonconductive sulfates (Townley and Winnick, 1981); $LiCrO_2$ appeared as a suitable substitute. When the electrolyte was changed to $K_2S_2O_7$, a more conductive electrode was needed, due to the lower operating temperature. Scott (1985) chose a porous perovskite ceramic of $La_{0.8}Sr_{0.2}CoO_3$ and found it to be both conductive and stable in the corrosive cell environment. These electrodes were formed by sintering the proper sized particles at 1,100°C in a procedure optimized by Franke and Winnick (1989b). These perovskites were compared with NiO electrodes in the MCFC and were found to have similar overall kinetics.

During longer duration experiments in the SO_x removal cell by the present researchers, a decrease in performance, not attributable to electrode pore flooding, was detected. X-ray analysis of the post-run electrodes showed formation of the sulfates of each of the perovskite components (La, Sr and Co sulfates). These reaction products are nonconductive and reduce the available sites for electrochemical reaction. As part of this work, lithiated nickel oxide was identified as a superior material for both anode and cathode electrodes, providing low polarization while remaining chemically stable (McHenry and Winnick, 1993).

Theory and Design

It is anticipated that, in a commercial design, removal flux of SO_x, and hence *effective* current density:

$$i = 2FN$$

that is, on a *superficial-area* basis, would be limited by diffusional transport of SO_3 to the gas/electrolyte interface. This limitation is directly calculable from available correlations for mass transfer to a flat plate in a laminar flow rectangular or triangular channel (Incropera and DeWitt, 1985). These calculations lead to an estimate of about 500 A/m^2 (50 mA/cm^2) for SO_3 transport, assuming 90% removal. At a flue gas velocity of 24 m/s (79 ft/s), the mass-transfer coefficient is about 0.12 m/s; the pressure drop in a 1.2 m (4 ft) long triangular channel of 4.2 mm^2 cross-sectional area would be about 2,600 Pa (10 in. of water), which is well below that encountered in liquid (for example, limestone slurry) scrubbers, about 7,800 Pa (30 in. of water).

The driving force for the SO_x removal is provided by the applied voltage, which must be kept to a minimum for the process to be economically attractive. The ionic migration through a thin (<1 mm) membrane at these temperatures (~400°C) will require negligible polarization (Appleby and Foulkes, 1989b). The polarization at each electrode required by the electrochemical reactions (activation overpotential) is represented by the Butler-Volmer equation in the approximate Tafel form:

$$i_{an} = i_o e^{\alpha_{an}\eta_{an}f} \tag{7a}$$

$$i_{ca} = i_o e^{-\alpha_{ca}\eta_{ca}f} \tag{7b}$$

where the current density is on a *true* electrode-electrolyte area basis. Experiments on flat-plate electrodes in molten electrolyte (Scott, 1985) provided quantitative results for the parameters needed in the equation:

$$i_0 = 300 \text{ A/m}^2, \quad \alpha_{an} = 1, \quad \alpha_{ca} = 1$$

With these values, the activation polarization in a full cell with porous electrodes can be estimated: even with no area enhancement (true area/superficial area = 1), the voltage needed at 500 A/m^2 is 0.038 V at each electrode, well within the required economic window. However, Franke found, in a full cell experiment, that i_0 was *apparently* three orders of magnitude lower (Franke and Winnick, 1989b). If the pores in the electrode are flooded, the active area for gas-electrolyte-electrode contact is minimized. In fact, with minimal gas-electrolyte surface, as would be the case with flooded pores, the electrochemical reduction in pyrosulfate will proceed, Eq. 1, producing sulfate ions; but the reaction of sulfate with incoming SO_3 will be curtailed, and the sulfate concentration will quickly build beyond its solubility limit in the pyrosulfate electrolyte. When

partial solidification occurs at the electrode-electrolyte interface, where the sulfate is formed, the polarization will rise, indicating low effective exchange current densities. In actuality, the increased polarization is due to both concentration and ohmic effects for the reasons just described.

It is thus crucial to avoid flooding of the electrode pores; improved membrane construction with increased membrane capillarity was expected to improve the effective exchange current density and, hence, lower polarizations in full-cell tests.

It is also necessary to maintain electronic conduction through the electrodes. Bare nickel failed to remain conductive in early tests at 600°C in the ternary sulfate eutectic, with complete reaction to $NiSO_4$. Thermodynamic phase equilibria calculations (Barin and Knacke, 1977) of the Ni-SO_2-O_2 system showed the preferred phase to be $NiSO_4$ at both 600°C and 400°C. The use of lithium oxide to fill cation vacancies would upset this equilibrium, as cation vacancies are required for oxidation of Ni. Other researchers (Wise and Oudar, 1990) and (Evans, 1981) have shown that the inclusion of LiO vapors in the gas phase retards the oxidation of Ni and increase the electronic conductivity of the resulting oxide. The nickel oxide can also be doped with LiO prior to exposure in the electrochemical cell.

Since no experiments had been performed on the use of lithiated nickel oxide in an SO_3 atmosphere, the suitability of this material as an electrode was investigated (McHenry and Winnick, 1993). Tests of candidate matrix materials were conducted to prove chemical stability. Full cell studies were required to establish the improvements caused by new membrane matrix materials and fabrication techniques.

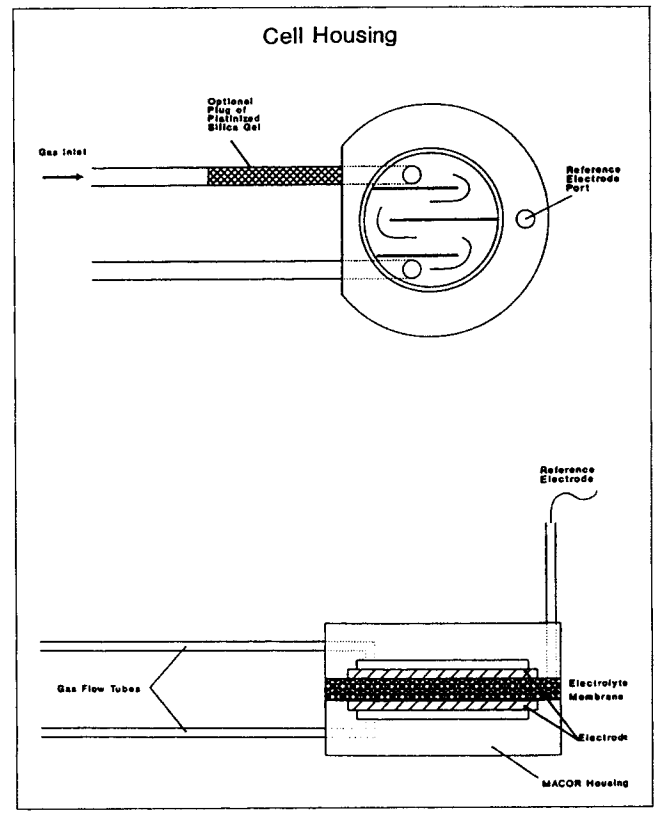

Figure 2. Electrochemical SO_x removal cell.

Experimental Studies

With the $K_2Mg_2(SO_4)_3$ membranes showing insufficient electrolyte retention, a search was begun for a new matrix material. Free energy calculations of possible reactions between electrolyte and matrix material identified several candidates, including borosilicate glass, titania, zirconia, silicon carbide and silicon nitride.

Chemical stability testing of the candidate matrix materials was carried out by soaking the material in molten $K_2S_2O_7$ at 400°C for one week. Due to the small particle size and high surface area, reaction, if favorable, should occur quickly. The reaction products were analyzed by X-ray powder diffraction in a Philips Model PW 1800 Automatic Powder Diffractometer with phase identification by the accompanying software.

The lithiated NiO electrodes were prepared from commercially available Ni sheets, 1.25-mm-thick National Standard Fibrex mesh. The material was cut to a diameter such that, after the volume change upon oxidation, the electrodes would fill the electrode well in the housings. The disks were dipped in a LiOH solution and dried at 120°C, placed in the housings and oxidized at 575°C.

A bench-scale cell has been used to demonstrate the effectiveness of the removal process (Figure 2). The full cell consists of 0.075 m (3 in.) diameter cathode and anode housings with their respective electrodes and membrane sandwiched between the two halves. The ceramic housings are machined from Macor to provide a baffled gas-flow channel under the well for the electrode. The baffles are treated with platinum to provide current distribution. Gas enters the cell through a long glass tube filled with the platinized silica gel and exits the cell through an alumina tube. The glass tube is long enough to permit heating of the gas before it enters the preoxidation catalyst bed, assuring conversion from SO_2 to SO_3. Both tubes are cemented into the housing gas inlets to provide gas-tight construction.

The housings are machined to retain an electrode disk approximately one mm thick with a geometric area of 0.002 m^2. Electrical contact with the electrodes is provided by platinum wires (spliced to gold), which enter through the gas outlet tubes. The top housing also has a hole drilled in it for the reference electrode: a platinum wire inside an alumina tube with a gas atmosphere of the same composition at that fed to the cathode. The inside of the alumina tube is platinized, and in combination with the wire, acts to completely oxidize the SO_2.

The electrolyte membrane consists of $K_2S_2O_7$ (with 5 wt. % V_2O_5) retained in the interstices of an inert ceramic matrix. Initial membranes tested in the present investigation were hot-pressed, using MgO as the matrix precursor. Another membrane fabrication method has been developed, using tape casting to produce thin, flexible tapes of ceramic to which electrolyte is later added. Polymeric binder systems of vinyl butyral in toluene/ethanol with extra surfactant (Metoramic Sciences, Inc., Carlsbad, CA) were used to disperse and suspend the ceramic particles. The dispersion was sonicated and poured on a suitable substrate to form the "green" tape of ceramic. When added to the cell, the cell was heated in an atmosphere of 100% O_2 to burn the polymer. This procedure left a good distribution of pores between the ceramic particles.

To conduct full-cell experiments, the assembled cell was placed in a custom-built furnace, with temperature control

provided by a Barber-Coleman Model 122B controller connected to a double-pole solenoid. This arrangement allowed temperature control to within ±2°C. A PAR 371 potentiostat/galvanostat with Model 178 electrometer probe was used to control current applied to the cell. Cell potentials were monitored with Simpson Model 460 or Fluke Model 8050A or 8010A multimeters.

Simulated flue gas (Matheson) at approximately 0.3% SO_2, 3% O_2 in N_2 was fed to both the anode and cathode cell compartments. A plug of platinized silica gel was placed in the cell inlet tubes to oxidize SO_2. SO_2 concentrations were monitored with a Hewlett-Packard Model 5840A gas chromatograph and thermal conductivity detector. SO_x concentrations in the effluent were monitored by absorbing the effluent gas in 2% H_2O_2 and quantitatively determining sulfate content with a Dionex Model 100 Ion Chromatograph. SO_3 levels were calculated from the difference in SO_x and SO_2 concentrations. Calibration showed reproducible readings with an error of less than 5%.

Experimental Results

Chemical stability of matrix materials

Chemical stability of the matrices was determined by X-ray diffraction of reaction products from the treatment in $K_2S_2O_7$ and a comparison of the product and reactant scans. The software allowed the reactant patterns to be subtracted from the product patterns to determine if new phases were present. It should be noted that raw $K_2S_2O_7$ partially decomposed to K_2SO_4 and SO_3, according to the equilibrium reaction:

$$K_2S_2O_7 \rightleftharpoons K_2SO_4 + SO_3: \quad K_{eq} = 2 \times 10^{-6} \text{ at } 400°C \qquad (8)$$

due to the low partial pressure of SO_3 above the reaction mixture.

MgO was found to react to $K_2Mg_2(SO_4)_3$ (Franke, 1988). The borosilicate samples showed small amounts of $K_2Al(SO_4)_3$, a reaction product of Al_2O_3 contamination from the ball-milling step. Amorphous glass phases could not be determined. Titania and zirconia, along with all silicon carbide and nitride samples, were stable.

Ideal matrix particle sizes should be at least an order of magnitude smaller than the electrode pores, so that the resulting interstices in a close-packed matrix produce pores the size of the particles. Silicon carbide and nitride powders were determined to have appropriate distributions (Gerhold, 1990). All other materials were dropped from further consideration due to their particle-size distributions and availability.

Membrane fabrication

Several binder systems were evaluated for use in the tape-casting procedure. A mixture of methyl cellulose in water, with plasticizers of polyethylene glycol (MW = 10,000) or polyethylene oxide (MW = 900,000), was used to disperse the borosilicate glass matrix. Difficulties with drying rate were solved by covering the tape to maintain a partial pressure of solvent over the tape. If the drying rate is too slow with this binder solution, settling of the ceramic occurs. Thin (0.1 mm) tapes were produced and tested in the full cell, with binder removal before electrolyte addition, the preferred technique.

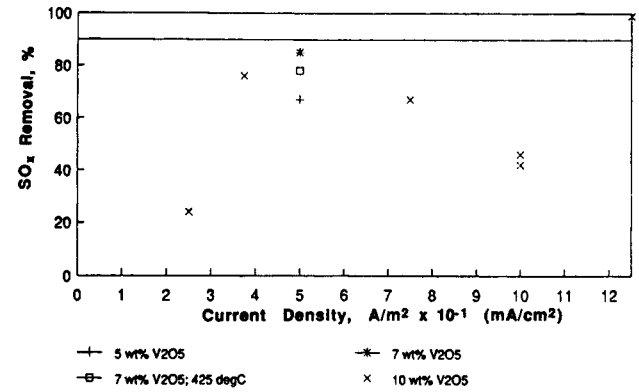

Figure 3. Cathodic removal of SO_3 after 10 min applied current.

Flow equal to that required for 90% removal at applied current.

Several binder systems are available in the commercial market. A polyvinyl butyral in the toluene/ethanol system from Metoramic Sciences, Inc. has been extensively used to produce homogeneous tapes of silicon nitride. Proper selection of substrate was crucial during high ambient humidity conditions. At present, tapes are made by combining a volume fraction of ceramic with the binder system, some excess surfactant and solvent, and milling for 12–24 h. The mix is then sonicated to break up agglomerates of ceramic. With proper drying rate control, thin (0.4 mm) tapes were produced and trimmed to 3-in. dia. All tapes were pressed at 83 bar (1,200 psi) to remove voids. If thicker tapes were desired, they were produced by laminating several tapes together. All of these structures, when tested in the full cell, formed good seals around the housing periphery and prevented gas crossover when sufficient electrolyte was retained in the membrane.

Full cell testing

Full cell tests were conducted under constant current conditions, with the applied current less than or equal to 100% stoichiometric removal. The runs detailed here all used lithiated NiO electrodes and tape cast membranes. All removal and polarization studies showed a time dependence of approach to steady state; polarization performance generally decreased at the cathode with increasing time, while removal increased as the experiment proceeded. The actual removal reaction requires a reagent to be generated at the cathode and then diffuse to the gas/liquid interface. This reagent, SO_4^{2-}, brings the cathode potential more negative.

With applied current equal to 90% stoichiometric removal, cathodic removal of SO_3 reached 90% or greater, given adequate time. Several levels of V_2O_5 electrolyte loading were used, for reasons explained below. Figure 3 shows removal data after ten minutes of applied current. The data point at 125 A/m^2 was obtained by following a different current path (50 A/m^2 = 36% removal for 2 h, 100 A/m^2 = 72% removal for 2 h, then 125 A/m^2). Figure 4 shows removal data for the same runs, but after 1 h. Removal is seen to be near 90%, in accordance with stoichiometry, for most currents, within the bounds of experimental error. Removal in excess of stoichiometry may be due to reaction with sulfate ions which have accumulated since

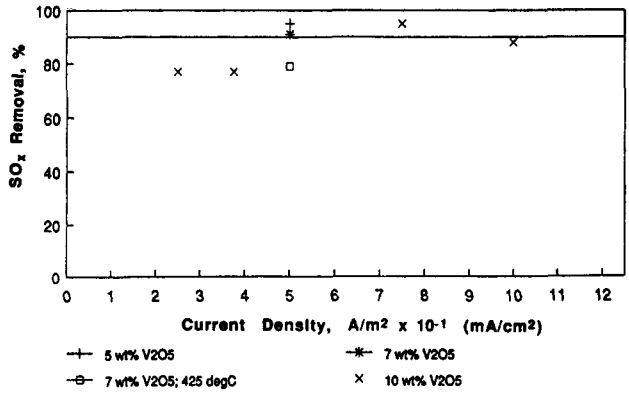

Figure 4. Cathodic removal of SO_3 after 60 min applied current.

Flow equal to that required for 90% removal at applied current.

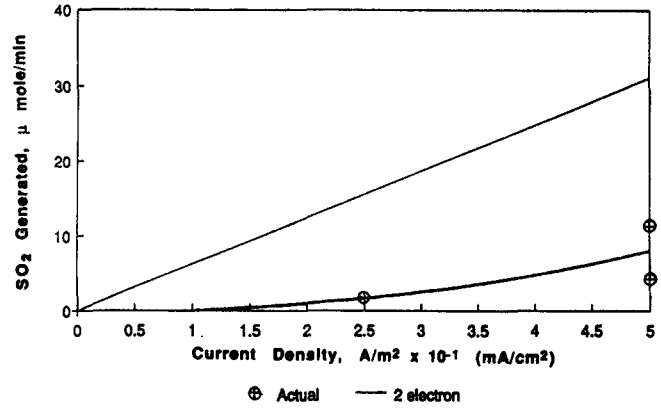

Figure 6. Cathodic SO_2 generation with applied current.

Flow equal to that required for 90% removal at applied current. 5 wt. % V_2O_5 in electrolyte.

current was applied, during the periods of lower removal, but is not outside the experimental error.

Looking at removal rates for 690×10^{-6} m^3/min of cathode gas, excess removal above the stoichiometric level is seen for all applied currents in Figure 5. This is due to excess sulfate in the electrolyte which is quickly neutralized by any SO_3 present in the gas phase.

With the present configuration, a new phenomenon was observed. As current was applied, SO_2 was seen to exit the cathode, as shown in Figure 6. This is possible from the electrochemistry of the system, as seen by Scott et al. (1988) in free electrolyte, but had not been observed before in high-surface-area-electrode, full-cell tests. As current rises, SO_2 is generated at a faster rate, one which overcomes the rate of oxidation by V_2O_5 in the electrolyte. It appears that SO_2 diffuses out of the porous cathode before contact with V_2O_5 and is carried off by the passing gas stream. Calculations of outlet flow rates showed that one-half of the generated SO_2 is being oxidized by the V_2O_5 and removed at the cathode. As current increases, so does flow rate, but this dependence on SO_2 generation was not observed due to the small range of currents tested. To overcome the SO_2 generation problem, more V_2O_5 was added to the cell through the reference port. At 7 wt. % V_2O_5, three-quarters of the electrochemically generated SO_2 was oxidized and removed (see Figure 7). At 10 wt. % V_2O_5, approximately 5/8 of generated SO_2 was oxidized and removed, according to the slope of the line through the data with applied current (Figure 8). This rate of oxidation is less than that for the 7 wt. % V_2O_5 study, but two major differences were present. First, flow was continuously provided at a level such that 90% stoichiometric removal would occur at 125 A/m^2; SO_2 which escapes the electrolyte does not have sufficient residence time at the lower currents to diffuse back to the electrolyte. Second, SO_2 was present at zero current, showing that the preoxidation catalyst was not saturated with an equilibrium level of SO_2 at the start of the run.

At the anode, SO_3 generation is seen to deviate from stoichiometry at all V_2O_5 levels, Figures 9 and 10. This discrepancy can be explained by two causes. Gas leakage accounts for most of the discrepancy at the higher V_2O_5 and current levels. The second cause is attributed to residual sulfate ions accumulating at the anode, as seen by cathodic SO_2 generation data. When SO_2 is generated at the cathode and not oxidized and removed, excess sulfate ions accumulate in the electrolyte and migrate to the anode. At the anode, they are either oxidized or raise the melting point of the electrolyte to the point where the electrolyte freezes on the anode surfaces. Excess sulfate at the anode will absorb SO_3 and neutralize it to form the $S_2O_7^{2-}$ ion. This second phenomenon is confirmed by polarization data.

Polarization data for the full cell after 10 min of applied

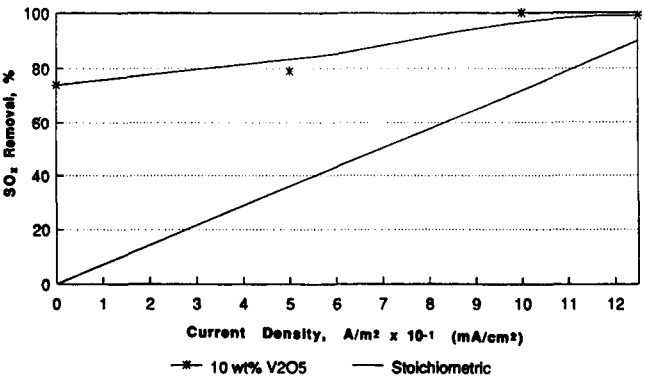

Figure 5. Cathodic removal of SO_3 with current.

Flow of 690×10^{-6} m^3/min of 0.31% SO_2, 3% O_2 in N_2 to cathode; all SO_2 oxidized to SO_3. Line represents stoichiometric removal.

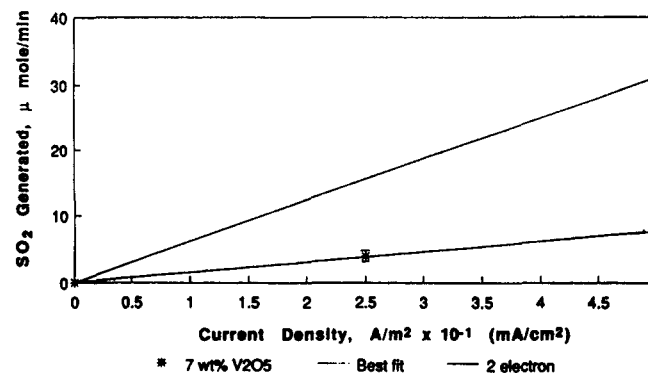

Figure 7. Cathodic SO_2 generation with applied current.

Flow equal to that required for 90% removal at applied current. 7 wt. % V_2O_5 in electrolyte.

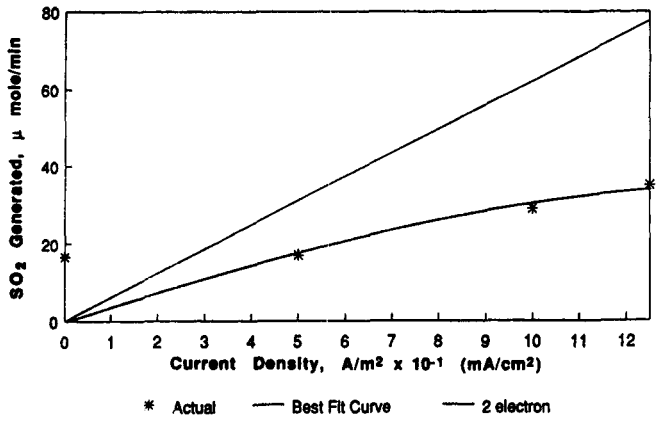

Figure 8. Cathodic SO_2 generation with applied current.

Flow for 90% removal at 125 A/m². 10 wt. % V_2O_5 in electrolyte.

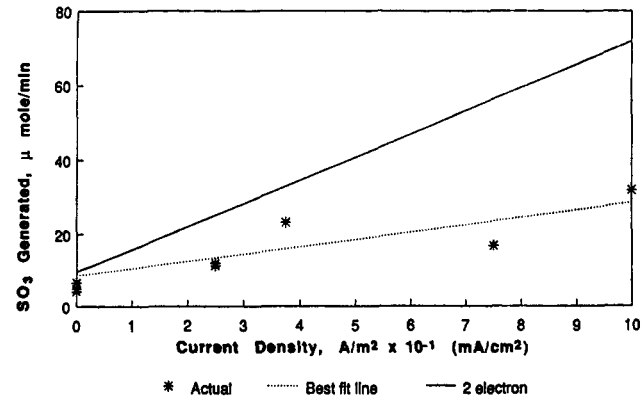

Figure 10. Anodic SO_3 generation, 10 wt. % V_2O_5 electrolyte.

Offset in calculated rates due to oxidation of SO_2 fed to anode.

current are exhibited in Figure 11. The effect of increasing V_2O_5 content is minimal after this short duration. After 1 h of applied current (Figure 12), a greater effect of V_2O_5 loading is observed. As V_2O_5 content increases, polarization decreases. The anodic polarization suffers from sulfate accumulation at the lower V_2O_5 loadings. This finding proves that increased vanadia loadings oxidize more of the cathodically-generated SO_2 before it can escape from the electrolyte.

Discussion

The results above show that the electrochemical process is capable of removing 90% of inlet SO_3, the product of the catalytic oxidation of SO_2. For all levels of V_2O_5 tested, removal reached greater than 80%, with removals in excess of 90% for 10 wt. % V_2O_5.

The greatest improvement found in the present configuration is in the area of polarization. Franke and Winnick (1989b) presented polarization data up to a maximum of 20 A/m² (0.04 A), with a cathodic overpotential of 2.7 V. The present curves show much higher current densities (10–20×) for the same or lower overpotential, but still 10–20 times lower than the design goal of 500 A/m² at 0.5 V (Franke and Winnick, 1989a). Analysis of the new polarization curves shows the *effective* exchange current density to change with V_2O_5 loading: 0.52 A/m² at 5 wt. % to 1.33 A/m² at 10 wt. %, the latter an improvement by a factor of four over the results of Franke. This improved polarization is due to a number of factors: First, the lithiated NiO electrodes remain stable during the run, compared to the perovskite used by Franke. And, second, the pores are larger in the NiO, reducing the level of electrode pore flooding and leaving more surface area exposed to gas than with the perovskite, even though the NiO possessed lower surface area.

The present removal cell configuration shows a much extended operating lifetime. Using tape cast membranes and lithiated nickel oxide electrodes, runs have been performed up to 28 days, with only minor degradation in electrolyte resistance and polarization. All of these runs were voluntarily terminated. Post-mortem analysis showed low levels of NiO corrosion products, which can be explained as above. Runs with perovskite electrodes and hot-pressed membranes typically produced quality data for 4 days, with an increase in electrolyte resistance and polarization during the run.

A new problem was detected in the above data. The release of SO_2 at the cathode showed insufficient V_2O_5 activity in the catholyte, allowing electrochemically-generated SO_2 to escape from the electrolyte and be carried away with the gas stream. Increasing the vanadia loading reduced this effect, but to an insufficient level to permit stoichiometric removal of inlet SO_x. It should be noted that in several of the runs, SO_3 concentra-

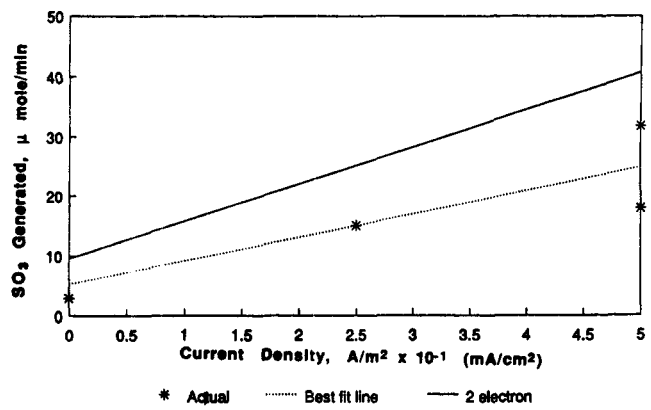

Figure 9. Anodic SO_3 generation, 5 wt. % V_2O_5 in electrolyte.

Offset in calculated rates due to oxidation of SO_2 fed to anode.

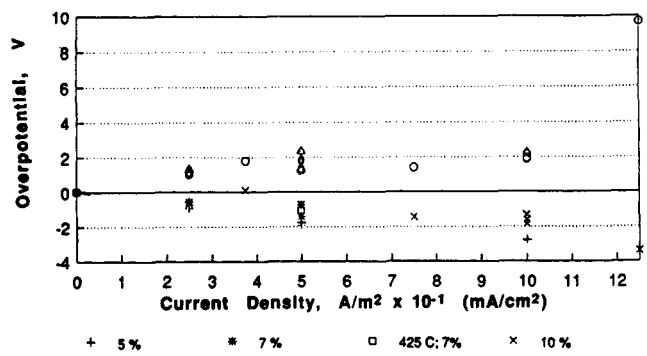

Figure 11. Polarization after 10 min applied current.

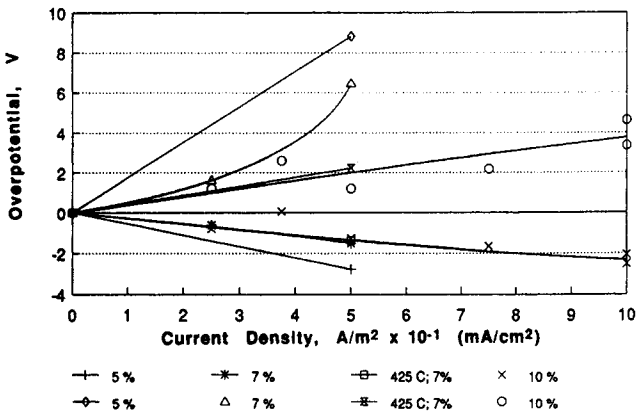

Figure 12. Polarization after 60 min applied current.

tions dropped to below the limits of detection, so that no SO_3 would be released during power plant operation. The problem of SO_2 release may be handled by optimizing the electrode structure such that the actual current density (not superficial) is reduced by one-half, which will in turn reduce the mass flux of SO_2 out of the electrode. Another option is to conduct the removal in stages, with intermediate oxidation of SO_2. These solutions require further study.

Design and Economic Analysis

To determine if this process is commercially feasible, a preliminary economic evaluation must be completed for a typical application. While the performance assumptions used in this evaluation have not been proven, they are within the range of performance that may be hoped for in the near future. A conceptual removal train was evaluated for a 500 MW_e coal-fired power plant, burning 3.5% sulfur coal, assuming 20% excess air, 35% thermodynamic efficiency, a 30-year lifetime and First Quarter, 1990 dollars.

The proposed full-scale design is envisioned as a bipolar stack of 700 repeating cells, each 4 ft^2 (0.4 m^2). For 90% removal of SO_2, a single set of stacks is needed, operating at 500 A/m^2 (46 A/ft^2), below the gas-phase mass-transfer limit, as detailed earlier. This requires a cell design such that gas velocities will provide large enough mass-transfer coefficients to support the mass flux.

Capital costs for the process are based on the latent estimate of MCFC stack costs (Appleby and Foulkes, 1989a), scaled on the basis of membrane area, at a cost of \$129/ft^2 (\$1,389/m^2). It is assumed that the stacks will have a ten-year operating lifetime, and require replacement twice during the operating lifetime. Additional capital items are the preoxidation reactor (\$5.5 million) and the oleum recovery plant (\$10.1 million).

Operating cost is primarily for electric power used at \$5 mil/kWh. The current demand is calculated directly from the rate of sulfur oxide removal, at 2 Faradays per mole: 11,670,000 A. If the voltage is estimated at 0.5 V, the power usage is about 1% of plant production. A modest revenue (\$100/ton) for the oleum product is taken to offset part of the operating costs.

A comparison shows the electrochemical process to offer a 50% savings in capital, relative to a limestone scrubbing operation (Burnett, 1983). In addition, levelized annual revenue requirements, which includes annual capital, operating and maintenance costs at \$3 million/kWh generated, show a savings of 80% over the conventional limestone scrubbing process, at \$18 million/kWh generated. Complete details are available in the references (Franke, 1988; McHenry, 1992).

Conclusions

The electrochemical membrane process for flue gas desulfurization has undergone substantial advancement. The process continues to show high rates and percentages of removal for SO_3 from the gas phase. Although SO_2 has recently been seen at the cathode, this may not present much of a problem with electrode optimization. By using a cathode with the proper surface area, diffusion of SO_2 out of the pores could be stopped and instead the SO_2 would be oxidized to SO_3 by the V_2O_5 in the electrolyte and removed, in accordance with cell chemistry. By changing to a new electrode material, lithiated NiO, polarization and cell lifetime have been increased by an order of magnitude.

Acknowledgment

The authors would like to thank the Department of Energy Pittsburgh Energy Technology Center for the financial support of this work. They also appreciate the donation of silicon carbide and silicon nitride materials by Phillips Petroleum.

Notation

f = F/RT
F = Faraday's constant, 96,500 C/equivalent
i = current density, A/m^2
i_0 = exchange current density, A/m^2
n = number of electrons
N = flux, $mol/cm^2 \cdot s$
R = gas constant
T = temperature, °C

Greek letters

α_{ca} = cathodic transfer coefficient
α_{an} = anodic transfer coefficient
η = overpotential, V

Literature Cited

Alexander, S., and J. Winnick, "Electrochemical Separation of Hydrogen Sulfide from Natural Gas," *Sep. Sci. & Tech.*, **25**, 2057 (1990).

Appleby, A. J., and F. R. Foulkes, *Fuel Cell Handbook*, Van Nostrand Reinhold, New York, p. 575 (1989a).

Appleby, A. J., and F. R. Foulkes, *Fuel Cell Handbook*, Van Nostrand Reinhold, New York, p. 000 (1989b).

Arendt, R. H., and M. J. Curran, "Alternate Fabrication Process for Molten Carbonate Fuel Cell Electrolyte Structures," *J. Electrochem. Soc.*, **127**, 1663 (1980).

Arendt, R. H., "Alternate Matrix Material for Molten Carbonate Fuel Cell Cathode," *J. Electrochem. Soc.*, **129**, 979 (1982).

Barin, I., and O. Knacke, *Thermochemical Properties of Inorganic Substances and Supplement*, Springer-Verlag, Berlin (1977).

Burnett, T. A., "Economic Evaluation of Limestone and Lime Flue Gas Desulfurization Processes," U.S. EPA Report 600/7-83-029 (1983).

Evans, U. R., *An Introduction to Metallic Corrosion*, 3rd ed., Edward Arnold, London (1981).

Franke, M. D., "Electrochemical Flue Gas Clean-up," PhD Diss., Georgia Institute of Technology (1988).

Franke, M. D., and J. Winnick, "The Electrochemistry of Molten $K_2S_2O_7 + K_2SO_4 + V_2O_5$," *J. Electroanal. Chem.*, **263**, 163 (1987).
Franke, M. D., and J. Winnick, "Membrane Separation of Sulfur Oxides from Hot Gas," *Ind. Eng. Chem. Res.*, **28**, 1352 (1989a).
Franke, M. D., and J. Winnick, "High Performance Molten Carbonate Fuel Cell Cathode," *J. Appl. Electrochem.*, **19**, 1 (1989b).
Gerhold, B., "Particle Distribution in Silicon Carbide and Silicon Nitride Powders," internal report, Phillips Petroleum Co. (1990).
Incropera, F. D., and D. P. DeWitt, *Fundamentals of Heat and Mass Transfer*, 2nd ed., Wiley, New York, p. 398 (1985).
Kang, M. P., and J. Winnick, "Concentration of CO_2 by a High-Temperature Electrochemical Membrane Cell," *J. Appl. Electrochem.*, **15**, 431 (1985).
Langer, S. H., and R. G. Haldeman, "Electrolytic Separation and Purification of Oxygen from Gas Mixtures," *J. Phys. Chem.*, **68**, 962 (1964).
McHenry, D. J., "Development of an Electrochemical Membrane Process for Removal of SO_x/NO_x from Flue Gas," PhD Diss., Georgia Institute of Technology (1992).
McHenry, D. J., and J. Winnick, "Electrochemical Membrane SO_2 Separation: Nickel Oxide Electrode Performance," *J. Electrochem. Soc.*, in press (1993).
Scott, K. D., "Electrochemical Flue Gas Desulfurization," PhD Diss., Georgia Institute of Technology (1985).
Scott, K. D., T. Fannon, and J. Winnick, "Electrochemical Flue Gas Desulfurization: Reactions in a Pyrosulfate-based Electrolyte," *J. Electrochem. Soc.*, **135**, 563 (1988).
Scott, K. D., and J. Winnick, "Electrochemical Membrane Cell Design for Sulphur Dioxide Separation from Flue Gas," *Gas Separation and Purif.*, **2**, 23 (1988).
Townley, D., and J. Winnick, "Flue Gas Desulfurization using an Electrochemical Sulfur Oxide Concentrator," *Ind. Eng. Chem. Proc. Des. & Dev.*, **20**, 435 (1981).
Townley, D., and J. Winnick, "Electrochemial Concentrator for Flue Gas Desulfurization," *Electrochim. Acta*, **28**, 389 (1983).
Walke, L., K. Atkinson, D. Clark, D. Scardaville, and J. Winnick, "Recovery of Carbon Dioxide from Flue Gas using an Electrochemical Membrane," *Gas Sep. and Purif.*, **2**, 72 (1988).
Weaver, D., and J. Winnick, "Evaluation of Cathode Materials for the Electrochemical Membrane H_2S Separator," *J. Electrochem. Soc.*, **138**, 1626 (1991).
Wise, H., and J. Oudar, *Material Concepts in Surface Reactivity and Catalysis*, Academic Press, San Diego, p. 233 (1981).

Manuscript received Nov. 12, 1992, and revision received June 7, 1993.